FERMILAB-Conf-03/397-E January 2004

THE CDF SILICON VERTEX DETECTOR FOR RUN II

R. ROSSIN
On behalf of the CDF collaboration
INFN Padova - Dipartimento di Fisica di Padova, Universita' di Padova
Via Marzolo 8, 35131 Padova - Italy
E-mail:rossin@fnal.gov

The 8 layer, 720k channel CDF Run II silicon detector is an essential part of the heavy flavor tagging and forward tracking capabilities of the CDF experiment. A summary of the experience in commissioning and operating this double-sided detector during the first 2 years of Run II is presented. The performances of the silicon in term of resolution, efficiency are also described. The results of the studies of radiation damage and the expected operational limits are discussed. A short description of the SVT, the Level 2 Silicon Vertex Trigger, one of the mayor upgrades related to the new silicon device is also presented. Finally, some of the many physics results achieved by means of the new Silicon+SVT machinery are also reviewed.

1 The CDF detector

The CDF II is a multi purpose experiment, with a very broad physics program. It's installed at Tevatron which is a $p\bar{p}$ collider with $\sqrt{s}$=1.96 TeV, the bunch time interval is 396 ns (36+36 bunches) and the luminosity around 10^{32} $cm^{-2}s^{-1}$. The detector has a rather classic design; from the beam line to outside there is a silicon tracking device, then a fast drift central chamber (Central Outer Tracker) inside a magnetic field of 1.4 T, which provides efficient track reconstruction up to $|\eta|=1$, precise transverse momentum measurement, 0.1% at 1 GeV, and a single hit resolution of about 150 μm. Outside the solenoid are placed the electromagnetic and hadron calorimeters and then the muon chambers. A complete description of the apparatus can be found in the Technical Design Report [1].

2 The Silicon tracker

The Silicon Detector is a high-precision microstrip tracker that provides information on both r - ϕ and z views. It consists of 7 layers in the central region ($|\eta|<1$) and 8 in the forward ($1<|\eta|<2$), for a total of about 720000 channels which guarantees an efficient coverage up to $|z|\sim50$ cm along the beam axis, around the nominal interaction point. The silicon apparatus is physically divided into 3 subsystems.

The innermost is Layer 00 (L00), it is a single sided single layer silicon device mounted directly onto the beam pipe with an almost 12 fold azimuthal symmetry. It has been installed in order to improve impact parameter resolution and b-tagging capabilities. It provides one single, high precision point measurement before track scattering. Sensors have a 25 μm pitch with a 50 μm readout. L00 is a low mass detector with lightweight fine-pitch kapton cables which allow the whole front-end electronics to be mounted outside the tracking volume. It has been designed to survive to the high radiation present at ~1.5 cm from the interaction region.[2]

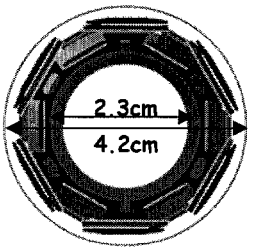

Figure 1. L00 section. Visible is the castellated structure with inner (128 strip) and outer (256 strip) sensors.

SVXII is the core of the silicon tracking system. It's a 5 double sided layers detector with three double metal 90° layers and two 1.2° layers, distributed in between 2.5 and 10.6 cm radii. It is used for vertexing and triggering when linked to COT tracks. Trigger functionality imposes very strict requirement on the alignment of the detector, less than 100 μrad, requirement that has been even exceeded during the assembly. This detector, very symmetric, has a 12 fold azimuthal structure, in the plane orthogonal to the beam (r - ϕ), and a 6 fold electrical structure in the beam direction (z direction). This symmetry has strongly been exploited by the displaced track trigger.

In between the central drift chamber and the main silicon tracker lies the Intermediate Silicon Layer (ISL). It's a double sided small angle stereo (1.2°) detector with 1 central layer up to $|\eta|=1$, which helps to extrapolate tracks from the COT into the silicon, and 2 layers in the region $1<|\eta|<2$ to increase the tracking acceptance in the forward region where the drift chamber doesn't cover efficiently. The total length of this detector is about 190 cm. ISL has a simpler design with respect to SVX (one flavor of silicon sensors, electronics mounted off silicon) and since it's not used in the trigger system it doesn't require a strict alignment.

All the silicon sensors are readout by means of the same SVX3D chip. Each chip has 128 channels, there are more than 5600 chips. A chip can be logically divided into an analog and a digital section. The analog section has, for each of the 128 channels, a FE low noise integrator followed by a 46 cell analog pipeline with 4 buffer cells, used to store the information while waiting for a Level 1 accept. The digital section has 8 bit ADC Wilkinson comparators, has a Dynamical Pedestal Subtraction (DPS) feature for common noise suppression, and after DPS has a sparsification logic to increase the readout speed. The chip operates in dead-timeless mode, which means that it's able to acquire and integrate while digitizing. It's designed to be compatible with 396/132 ns bunch spacing.[3]

2.1 Commissioning and operations

Due to its complexity, the commissioning of the detector took rather a long time. Figure 2 shows the percentage of the silicon system which has been biased and integrated versus time. It took about 1 ½ years to get to the final point, now the silicon is stable and about 90% is up and running. An incomplete list of issues encountered during the commissioning period will be discussed below.

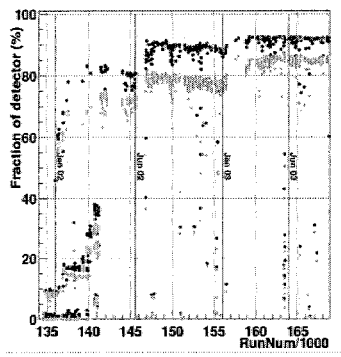

Figure 2. Percentage of operational ladders (black) and ladders with an error rate less than 1% (gray) versus time from the beginning of the commissioning.

2.1.1 L00 noise

When first turned on in CDF a significant coherent noise was observed on L00. This noise is characterized by non-uniform pedestal shape oscillation across the strips of a sensor that also changes on an event-by-event basis: it has been determined to be pickup on the fine-pitched cables. This prevent the DPS, which assumes a flat pedestal, from working. However, the small channel count of the L00 detector allows all strips to be readout and then fitted offline to polynomials on an event-by-event basis. A sample physics event before and after fitted pedestal subtraction is displayed in Figure 3. The most important, negative, consequence of this noise is that the sparsification must be disabled and so the time for the complete L00 readout prevents its insertion into the displaced track trigger.

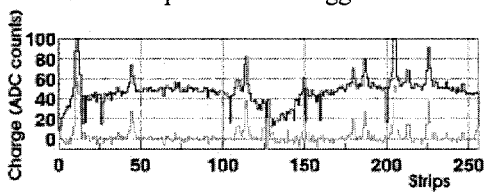

Figure 3. Sample physics event in a 256 strip L00 sensor. The raw charge is plotted in black, overlaid in gray is the pedestal subtracted charge.

2.1.2 Wirebond resonance

Another problem encountered is some spontaneous failures which looked like power loss to some chip during operations. It happened during anomalous trigger conditions induced either by dead-time tests or during SVX3D chip high occupancy situations (the all 4 buffer cells of the pipeline filled and a 5th Level 1 accept issued). Both the situations lead to synchronous trigger conditions and consequent synchronous current absorption which caused resonant Lorentz forces on the chip bonds which finally broke. Extensive studies have been performed on this; the resonance and the bond breakage have been obtained in

test conditions. A variety of filters have been implemented to avoid this in the future: the removal of spurious sources of the 5th Level 1 accept, the current swing minimization and a trigger inhibit on resonance.

2.1.3 Beam loss

Two separate beam losses caused high instantaneous particle flux (~10^7 MIPs/cm^2) inside CDF with consequent damage of nine SVX3D chips. The first was a consequence of a RF failure in the Tevatron which created a DC beam the kicker magnets sprayed through CDF. The second was due to a false triggering of the abort magnets. Counter-measures have been adopted to prevent further high dose-rate situations: a fast interlock aborts the beam before it is debunched if an RF failure occurs, collimators have been added to intercept aborted beam.

2.1.4 Other failures

There were other failures, most of them occurred early in the commissioning of the detector. Among them blockage of the ISL cooling lines, failures of the optical readout system and port cards. Most of the problems have been solved or limited by the effort of the silicon group.

2.2 Performances

The analog performance of the detector is excellent, a connected sensor guarantees a good charge collection and a clear signal and noise separation.

Table 1. Signal to noise ratio for the 3 silicon subsystems.

S:N	ϕ	z
L00	10:1	
SVX	14:1	12:1
ISL	12:1	12:1

The charge collection efficiency is higher than 99% and the double sided detectors will allow to use charge correlation for cluster matching and eventually for particle ID with the energy loss rate.

The "standard" silicon tracking is a COT seeded outside-inside algorithm which starts from the tracks reconstructed in the central drift chamber and swims them into the silicon performing a progressive road search. Thanks to the effort spent to optimize the pattern recognition and to find a good alignment the tracking efficiency is now higher than 90% in the ϕ side, with an intrinsic resolution on an SVX single hit of 9 μm. On the z side there is still some work to do, mainly alignment of the 90° detectors.

The impact parameter resolution is strongly related to the L00 performance. This device has been designed mainly to give an important contribution to the IP determination especially in the regions with more

material. This has been confirmed by the data. After the alignment of L00, there is a clear improvement in IP resolution in the silicon regions with passive material, in particular for tracks with low transverse momentum (Figure 4).

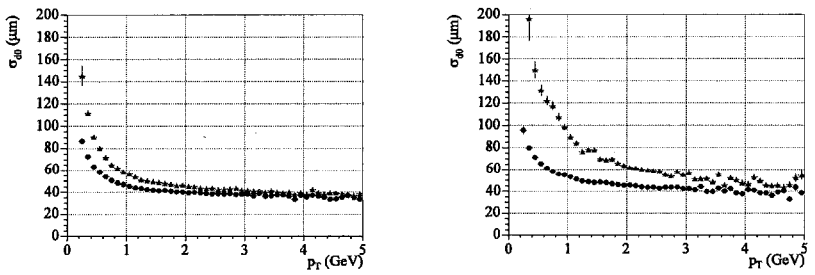

Figure 4. Impact parameter resolution versus transverse momentum for all tracks with $|\eta|<1$ in regions of the SVX which contain only silicon (left) and in regions of SVX which contain also the FE electronics (right). Bullets(triangles) represent the resolution with(without) the L00 information. The measured resolution contains also the contribution from the beam spot size (33 μm).

Besides the COT seeded tracking in the central region, the silicon can provide tracking coverage also in the forward region up to $|\eta|=2$. The tracking algorithm uses the energy cluster position and height in the Plug Calorimeter and the Primary Vertex position to calculate two seed tracks, two seeds because the charge identification will be provided by the silicon. These two seeds are then introduced as starting points into an Outside-In algorithm which proceeds in an analog manner as the standard one; the silicon hits are then associated to form a track. There is still some work to do in aligning the plug calorimeter but the performances are encouraging. Figure 5 shows that the calorimeter seeded - silicon tracking has an efficiency higher than 50% and the charge misidentification is less than 10% up to $|\eta|=2$.

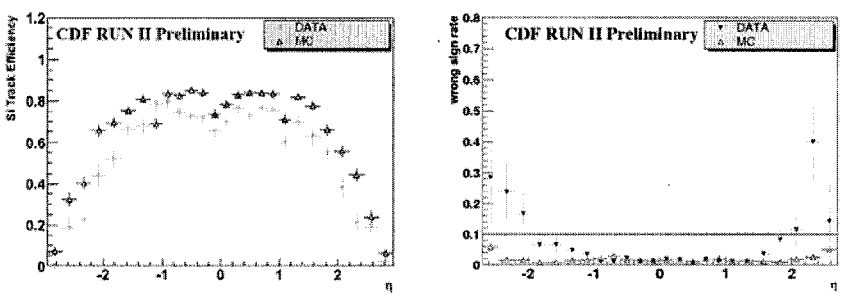

Figure 5. Efficiency (left) and charge misidentification rate (right) of the calorimeter-seeded algorithm. The performances have been evaluated on a sample of $Z \rightarrow e^+e^-$ with one electron reconstructed in the central drift chamber and the other in the calorimeter.

2.3 Radiation damage assessment

From the beginning of Run2 CDF integrated more than 250 pb^{-1} out of a total delivered luminosity from the Tevatron close to 350 pb^{-1}. A radiation damage assessment of the silicon has been performed using both dedicated dosimeters and the silicon detector itself. The data provided by approximately 1000 Thermal Luminescent Dosimeters installed inside the tracking region show a radial dependence which follows a power law in 1/r; at a radius of 3 cm from the beam, the silicon sensors accumulate radiation at a rate of 300±60 rad/pb^{-1}, in perfect agreement with Run1 data. The evaluations of radiation field from TLD measurements and the power law model have been compared to the radiation evaluated by the leakage current measurements, for instance on L00. Figure 5 shows a 10% agreement between these two independent evaluations. The conclusion that can be drawn from this work is that from radiation damage CDF silicon is expected to run up to 6 fb^{-1} of integrated luminosity.

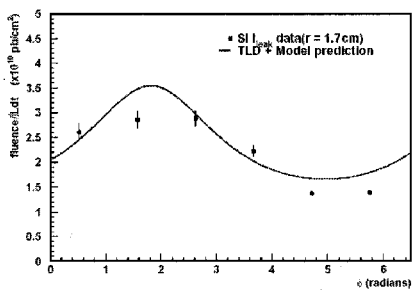

Figure 6. Fluence comparison between the TLD measurements extrapolated to the L00 radius by means of the $1/r^{\alpha}$ power law model and the evaluations from L00 the leakage currents. The azimuthal fluence dependence is due to the not centered beam with respect to the detector.

3 The Silicon Vertex Trigger

3.1 CDF trigger system

CDF has a three level trigger system which reduces the collision rate of 2.5 MHz to less than 70 Hz. The first stage is a synchronous pipeline of programmable logic and lookup tables which takes about 5.5 μs to take the decision, based on the existence of physics objects like electrons, muons or tracks. The approximate L1A rate is now 35 kHz. Trigger Level 2 is asynchronous: events remain in the buffer until they are accepted or rejected. Events are partially reconstructed and analyzed depending on the detector. Muons, electrons and jets are better defined. The Silicon Vertex Trigger (SVT)[4] operates at this level. Level 2 accept rate is around 350 Hz. After being accepted by Level 2 trigger the entire event is read and loaded into a farm of commercial CPU running the full offline reconstruction software. If

compared with the CDF Run1 trigger, this system is capable of about one order of magnitude higher than previous, the drift chamber tracking has been moved from Level 2 to Level 1 and the silicon tracking moved from offline to Level 2.

3.2 Level 1 track trigger

The drift chamber tracking in the trigger is essential for electron and muon identification and for the hadronic bottom and charm triggers. The COT is segmented into 4 axial and 4 stereo superlayers of 12 measurement layers each. The eXtremely Fast Tracker (XFT) processor works on the axial projection, orthogonal to the beam line, it begins classifying hits on each wire and then defines line segments. The 4 line segments in the 4 axial superlayers are put together to form a track candidate. The system is about 96% efficient for tracks of $p_t > 1.5$ GeV/c, does its work in 2 μs and achieves a resolution only about a factor 10 coarser than the final offline track resolution in measuring the momentum and the direction of the particle in the transverse plane ($\Delta p_t/p_t^2$=1.65% GeV^{-1} , $\Delta\phi_0$= 5.1 mrad).

3.3 The Level 2 silicon track trigger

High precision *b* physics measurements as B_S mixing demand fully reconstructed decays that are not achievable with leptonic trigger since the neutrino presence. Therefore, in order to have large samples of *b* completely reconstructed, it is desirable to collect hadronic *b* decays. The characteristic that can be exploited to separate, at trigger level, this signal from background is that tracks from *b* decay have an impact parameter significantly different from zero; following this idea CDF has built a trigger which selects *b* hadronic decays.

In order to accomplish that the silicon vertex trigger has to have an IP resolution comparable with the offline one (~35 μm) and has to do the job in 10-20 μs. To obtain this SVT takes advantage of the high degree of symmetry of the SVX detector to do everything can be done in parallel. The azimuthal symmetry of this detector about the beam axis is fully exploited as well as the 6 fold repetition of this detector along the beam axis; even the approximate radial symmetry from layer to layer is used, for example the clustering of pulse heights into charge centroids is done in 12x6x5=360 identical copies of the same chip, running the same algorithm. The online Silicon Vertex Tracker inputs are the list of COT tracks found by XFT and the data from four out of the five SVX axial silicon layers. The SVT core is organized as 12 identical systems (sectors). Figure 7 shows the

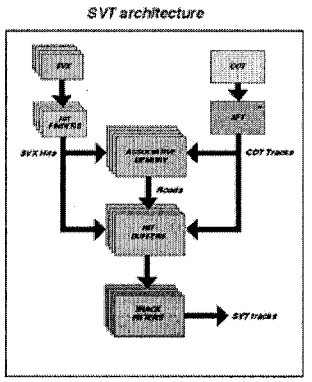

Figure 7. SVT components list and data flow.

architecture of one of these systems. At each beam crossing the silicon FE digitizes the charge induced on the strips and write these information in a pipeline waiting for a Level 1 accept. Each of the azimuthal slice is processes in a pipeline. The silicon information are sent to the Hit Finder, 3 per sector, which calculates the cluster centroid position of the silicon hits and sends them to the Hit Buffer, where they are stored for future reference, and to the Associative Memory (AM) units. Upon receiving the list of silicon centroids found by the Hit Finder and XFT tracks, each AM chip searches for all the coincidences which represent a legitimate particle trajectory (road). This is done by comparing the input data with a stored set of precalculated patterns. In order to limit the number of roads that would be needed to match all the possible tracks the AM system groups clusters into "superstrips" each covering about 250 μm. In this way the number of channels is reduced but the coarse resolution increases the number of fake tracks and may cause multiple candidates to fall within the same road. This width is a good compromise between cost, performances and processing time. For each Hit Buffer there are 2 AM boards with 128 chips each and 128 roads per chip which is about 32,000 roads. These predefined patterns have been generated with a Monte Carlo technique and the most probable have been written down. This gives a coverage of about 95%.
The AM boards are another example of parallel processing. They can be considered as a set of bingo cards, each chip is a bingo card with 128 lines and 5 entries per line, a bingo player raises the hand when he sees a set of five. This gives an algorithmic complexity which is linear in the number of hits coming in, and linear in the number of roads which have 5 hits.

Once selected the track candidates the last step is to perform the track fitting. In order to speed up the procedure the fitting problem has been linearized. Intersecting a circular track trajectory with a bunch of flat measurement planes doesn't give in general a linear relationship between circular parameters and the measured coordinates, but for tracks whose curvature and IP are not big the fitting problem can be linearized (this doesn't mean an approximation of a track with a straight line) which reduces the problem of doing least square fit to matrix multiplication. The coefficients of this matrix are derived from a linear regression to a large sample of MC data. This fast linearized fit gives as an output the Impact Parameter (d_0), the initial azimuthal direction (ϕ_0), transverse momentum (p_t) and a χ^2.

In term of time performance, from the Level 1 accepting an event to the delivering a list of silicon tracks to the Level 2 processor there is an average delay of 24 μs, the first 9 μs of which are spent waiting for the data to arrive. Figure 8 shows the SVT performance in term of IP resolution. The total width is given by the effective measurement resolution of 35 μm convoluted with the Tevatron intrinsic beam size of 33 μm. Cutting at 120 μm allows to be efficient for heavy flavor decays and reject about 90% of primary tracks. Requiring two such tracks gives about two order of magnitude rejection. The SVT efficiency

has been evaluated by using a sample of $J/\psi \rightarrow \mu\mu$ collected with the muon trigger. Figure 9 shows the efficiency as function of the track impact parameter. The plateau value is around 85% with a slow decrease over 1 mm. This behavior is due to a partially coverage of AM patterns over 1 mm.

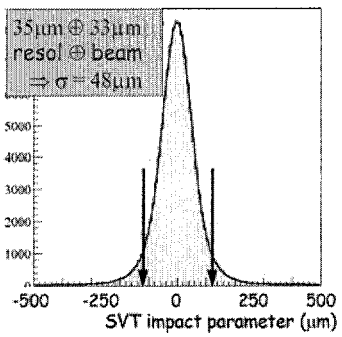

Figure 8. SVT Impact Parameter resolution.

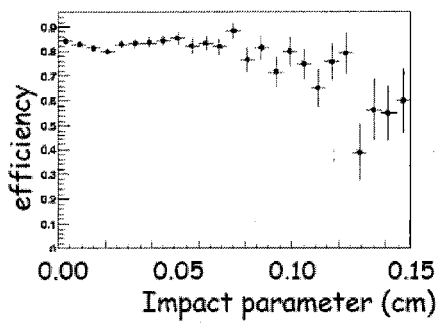

Figure 9. SVT efficiency versus Impact Parameter.

4 Physics results

The new trigger and the DAQ capabilities described before, together with the improved silicon detector reflect on the fact that CDF has been able to have new published physics out of even the first few months of data collected about two years ago[5]. That means that the new capabilities allow us to much better use the luminosity than in the past, even getting physics during the commissioning of the accelerator.

The new SVX capabilities allow CDF to repeat and improve the measurement yet done with Run1 data like *b*-flavored hadrons lifetimes measurements using the J/ψ dimuon trigger. Figure 10 shows an exclusive lifetime measurement of a B_S decaying into a 4 track final state.

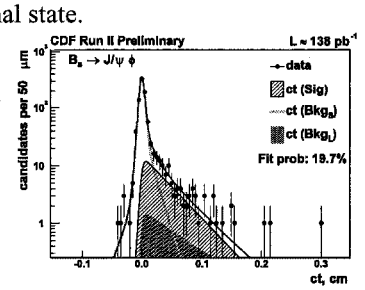

Figure 10. B_S exclusive lifetime measurement in the $B_S \rightarrow J/\Psi\ \phi$; $J/\Psi \rightarrow \mu\mu$; $\phi \rightarrow K^+K^-$ channel.

What instead is completely new, and never see before is the possibility to reconstruct large samples of fully hadronic *b* decays. This has been possible only because of the new displaced track trigger, the SVT. Figure 11 shows the only existing BR measurement of the $B_S \rightarrow D_S^-\pi^+; D_S^- \rightarrow \phi\pi^-; \phi \rightarrow K^+K^-$ channel.

This is a golden channel for the future B_S mixing measurement since it has a fully reconstructed and flavor defined final state.

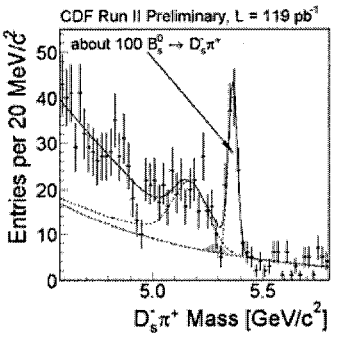

Figure 11. B_S invariant mass in the fully hadronic $B_S \to D_S\pi$; $D_S \to \phi\pi$; $\phi \to KK$ channel.

Measurement of forward-backward charge asymmetry in W production is one of the steps for a precise determination of the W mass. Tracking for forward leptons is the key component of this measurement since the sensitivity is maximum at high values of pseudorapidity. The tools are yet ready, the sensitivity achieved looking only to the electron sample is yet better than the Run1 sensitivity on the complete μ+e sample.

5 Conclusions

The complex design of the CDF Silicon Tracker implied a long and challenging commissioning period and will still need work on tuning the offline code for improving the performances and continuing maintenance to maximize the longevity of the detector. On overall the detector has been performing well and is operating stably since June 2002, the displaced tracks trigger being strongly boosting the physics capabilities of the experiment.

References

1. CDF Collaboration, "The CDF-II Detector Technical Design Report", *FERMILAB-Pub*-96-390-E.
2. T.K. Nelson for the CDF II Collaboration, "The CDF Layer 00 Detector", *FERMILAB-Conf*-01-357-E.
3. M. Garcia-Sciveres et al., "The SVX3D Integrated Circuit for Dead-timeless Silicon Strip Readout", *Nucl.Instrum.Meth.* **A435**:58-64 (1999)
4. W. Ashmanskas *et al.* "The CDF Silicon Vertex Trigger", *FERMILAB-Conf*-03-168-E.
5. CDF II Collaboration, "Measurement of the Mass Difference $M(D_S^+)$-$M(D^+)$ at CDF II", *FERMILAB-Pub*-03-048-E